ELSEVIER

Journal of Alloys and Compounds 340 (2002) 79–87

Journal of ALLOYS AND COMPOUNDS

www.elsevier.com/locate/jallcom

The effect of an electric field on the microstructural development during combustion synthesis of TiNi–TiC composites

Olivia A. Graeve[1], Zuhair A. Munir*

Department of Chemical Engineering and Materials Science, University of California, Davis, CA 95616, USA

Received 13 August 2001; received in revised form 16 October 2001; accepted 29 November 2001

Abstract

The role of an externally imposed (contacting) electric field on the microstructural development during the synthesis of TiC–TiNi composites was investigated. Using elemental reactants, composites with 60 and 70 vol% TiNi were synthesized by the self-propagating combustion method. The field had a direct effect on the velocity and temperature of the combustion wave, and had an influence on the particle size of the TiC phase formed within the TiNi matrix. The average particle size increased by at least a factor of two (from about 2.5 to 5.5 μm for the 60 vol% TiNi samples and from 1.5 to 3.0 μm for the 70 vol% TiNi samples) as the field strength was increased from zero to about 5 V cm^{-1}. Although higher temperatures and wave velocities result in higher temperature gradients and thus an anticipation of shorter residence time at the highest temperatures, the presence of a liquid phase has apparently a more direct effect on TiC particle growth. In cases where no liquid is present the results are different, as will be reported in a subsequent paper.

Keywords: Composites; Combustion synthesis

1. Introduction

Because of limitations stemming from thermodynamic and kinetic criteria, self-propagating combustion reactions are not possible in certain synthesis systems. These limitations include a low reaction enthalpy, a non-optimum thermal conductivity, and a low reaction rate [1]. Because of these limitations a fairly large number of materials systems cannot be synthesized by this method, including many intermetallics and composites. Among the methods of overcoming these limitations by activation, the use of an electric field has been shown to be highly effective [2–4]. The effect of the field can be thermal [5], providing an additional energy at a rate of σE^2 (σ being the electrical conductivity and E is the field), or it can include other contributions such as electromigration effects [6]. These effects are manifested by significant changes in the dynamics of self-propagating reactions. The application of the field has been shown to increase the temperature and rate of the reaction and influence the mechanism, and hence the nature and composition of the product [7–10]. Furthermore, there is evidence that the field has a role in the microstructural development of the product, exerting an influence on the grain size of the product [11].

In this paper we report the results of an investigation on the influence of the field on the microstructural development during the formation of TiNi–TiC composites. The choice of this system was based on two considerations: (a) that the material can be synthesized without the application of an electric field and (b) that the amount of molten phases during the reaction can be varied. The first consideration makes possible the comparison between field-free and with field microstructures and the second enables us to determine the role of a molten phase in the microstructural development. The synthesis was accomplished according to:

$$2.11\text{Ti} + 1.11\text{Ni} + \text{C} \rightarrow \text{TiC} + 1.11\text{TiNi} \quad (1)$$

$$2.73\text{Ti} + 1.73\text{Ni} + \text{C} \rightarrow \text{TiC} + 1.73\text{TiNi} \quad (2)$$

Reactions (1) and (2) result in products containing the metallic component TiNi at 60 and 70 vol%, respectively. Table 1 shows selected properties for the two reaction

*Corresponding author. Tel.: +1-916-752-0400; fax: +1-916-752-1031.

E-mail address: zamunir@ucdavis.edu (Z.A. Munir).

[1]Current address: Department of Chemical and Materials Engineering, San Jose State University, One Washington Square, San Jose, CA 95192-0082.

0925-8388/02/$ – see front matter
PII: S0925-8388(02)00020-8

Table 1
Reaction characteristics

Reactants	Melting point of reactants (K)	Products (mol)		Adiabatic T (K)	
		60 vol%	70 vol%	60 vol%	70 vol%
Ni	1728	TiNi: 1.11	TiNi: 1.73	2375	2159
Ti	1693	TiC: 1.00	TiC: 1.00		
C	4100 (sublim.)				

systems investigated. The two reactions are highly exothermic with high adiabatic temperatures.

There are only few literature accounts on the synthesis of TiNi–TiC composites. Huang et al. [12,13] investigated the formation of TiNi–TiC composites by mechanical alloying. Powders of Ti, C, and Ni, milled in a planetary ball mill, fully reacted after 3 h and 35 min, forming a mixture of TiC and TiNi. The authors concluded that mechanical alloying is not governed by a gradual diffusional reaction but by a self-propagating high-temperature synthesis (SHS) reaction. The SHS reaction was believed to be triggered by the release of the heat of formation of TiC and ignited by the mechanical collisions. In another study, composites of TiC–TiNi were formed by sintering of the two components [14]. The focus of this work was the mechanical characterization of the composite and it was shown that TiC particles significantly enhance the wear resistance of TiNi.

The formation of the related composites of TiC–Ni by SHS has been investigated in considerable detail. This cermet is proposed as a substitute for WC–Co for use in cutting tools. Dunmead et al. [15] found that when combusting Ti+C+25wt%Ni to obtain TiC+25wt%Ni the reaction is controlled by the dissolution of carbon into a Ti–Ni melt with an apparent activation energy of 133 ± 50 kJ mol^{-1}. The product is formed by precipitation of TiC particles from the melt. Capaldi and Wood [16] reported an activation energy of 159 ± 42 kJ mol^{-1} and proposed the following stages for the formation of the composite: melting of Ti and Ni, initial reaction to form an intermetallic, reaction of remaining Ti to give TiC, and reaction of the intermetallic with remaining carbon to give the final product of TiC in a nickel matrix.

Using time-resolved X-ray diffraction Wong et al. [17] found that the first step in the combustion of Ti+C+25wt%Ni was the melting of titanium and nickel particles. Within 200 ms of melting, the titanium reacted with the solid carbon to form TiC. The total reaction time for the formation of the TiC was 0.4 ± 0.2 s. In addition, these authors detected Ni_3Ti and NiTi in the final product. Rogachev et al. [18] examined quenched fronts of a Ti+C+20at%Ni mixture reactions, and observed melting in agreement with the work of Wong, et al. [17]. The metallic melt, consisting of Ti and Ni, envelops the carbon particles. The minimum diameter of TiC particles found in the product was comparable to the particle size of the carbon particles (around 1 μm). They also found that nickel has an effect on the final composition of the combustion product: the addition of nickel leads to a shift in the titanium carbide composition closer to stoichiometry as compared to the Ti/C ratio in the original mixture.

The observations of LaSalvia and co-workers [19–21] showed that the microstructure for the TiC–Ni consisted of spheroidal TiC particles embedded in a nearly continuous Ni matrix. The TiC particles exhibited multiple cusps which indicated that they actually consisted of agglomerates of smaller grains.

2. Experimental methods

The reactants indicated in Eqs. (1) and (2) are elemental powders whose characteristics are shown in Table 2. The carbon used is amorphous and contained significant amounts of volatile impurities which necessitated outgassing. Outgassing was done in a furnace at 300 °C in a flowing argon gas for 12 h. Stoichiometric mixtures of powders were dry-mixed for 12 h in a ball mill, using alumina balls in glass jars. Samples which were X-rayed after milling showed the presence of peaks corresponding to Ti and Ni only (the carbon is amorphous). While contamination of the reactants with small amounts of alumina is possible during this form of milling, it is believed not to play a significant role in the subsequent reaction process. We base these conclusions on the results of synchrotron radiation studies conducted on this system (E.M. Carrillo-Heian and Z.A. Munir, unpublished results).

Approximately 5.0 g of the mixed powder were uniaxially cold-pressed in a steel die to form round-ended rhombohedral compacts with an approximate height of 10 mm, a length of 21.7 mm, and a width of 6.8 mm. The applied force for the cold-pressing was 22 kN. No binders

Table 2
Reactant powder characteristics

Powder	Manufacturer	Purity (wt%)	Particle size
Ti	Alfa Aesar (Lot# B26G31)	99.0	−325 mesh
C	Cabot Corporation (Monarch 1300 amorphous)	98.9	13 nm (average)
Ni	Alfa Aesar (Lot# L15F07)	99.9	2.2–3.0 μm (2.5 μm average)

or solvents were used during mixing or pressing. The resulting compacts had relative densities of about 65%.

The compacts were then placed between graphite plates acting as electrodes inside a stainless steel combustion chamber. The combustion experiments were conducted under one atmosphere of argon gas. The electrodes were separated by the height of the sample and the wave propagated along the length of the sample. The reaction was ignited by heat radiated from a tungsten coil placed 2–3 mm from one end of the compact. A typical experiment begins by the imposition of a fixed AC voltage across the sample simultaneously with the activation of the tungsten ignition source. Once the reaction is initiated, the ignition coil is turned off immediately. The applied field is maintained by an AC (60 Hz line frequency) power supply with high current capability. The instantaneous current passing through the sample is measured by an inductance coil and the instantaneous voltage across the sample is measured directly. The temperature of the combustion wave is measured by a two-color pyrometer with a response time of 0.01 s. The pyrometer, with a spot size of 1 mm, is focused on the middle portion of the sample. The minimum temperature the pyrometer can read is 1400 °C. The measurements of temperature, current, and voltage are synchronized through a computerized data acquisition system. The displacement of the wave is recorded by means of a video recorder with a time-code generator.

X-ray diffraction (XRD) patterns of the samples were obtained using a Scintag XDS 2000 diffractometer with Cu Kα radiation and an Ni filter. The size and morphology of the particles were examined by an ISI-DS 130 scanning electron microscope (SEM) equipped with a secondary electron detector and a backscatter detector.

3. Results

An increase in the applied field results in an increase in the current, temperature, and wave velocity as seen in Fig. 1a–c, respectively. The wave velocity for both compositions increased by nearly a factor of three as the applied field increased from zero to 6 V cm^{-1}. Correspondingly, the maximum temperature increased by 446 and 487 °C for the 60 and 70 vol% samples, respectively. Since more heat is generated by the formation of TiC, the first reaction, Eq. (1), reached higher temperatures and wave velocities for any given electric field.

A typical X-ray diffraction pattern for a product is shown in Fig. 2. The observed peaks indicate the presence of the TiC and TiNi phases only. Fig. 3a is a typical micrograph for samples with 60 vol% TiNi reacted without the field. The dark round particles are TiC, and the lighter matrix is TiNi. Fig. 3b shows a sample with the same composition reacted under the influence of a field of 5.82 V cm^{-1}. A visual comparison shows that the sample reacted with the electric field has larger TiC particles. Both micrographs are from areas close to the middle of the samples.

In order to quantify the effect of the field on the microstructure of the resulting composites, a particle size analysis was performed using many SEM micrographs from each sample. The micrographs were taken from locations close to the middle of the samples in order to avoid end effects. The NIH Image software used for the analysis measures the particle area. The particle radius was later extracted by assuming that the particles were perfectly spherical. Fig. 3a,b shows that this assumption is reasonable. The particle radii were later assembled into frequency groups. The analysis was performed on five representative samples from each composition studied and the final results were assembled in Fig. 4a,b for the 60 and 70 vol% TiNi samples, respectively. As the applied voltage is increased the TiC particles shift to larger sizes and the distribution becomes broader. A plot of mean particle size of TiC as a function of the maximum reaction temperature is shown in Fig. 5. The mean was determined by assuming that the particles exhibited a normal distribution. The dashed line at the lower temperatures of Fig. 5 for the 70 vol% TiNi composite has been drawn in the graph as an extrapolation of the actual data. Fig. 4b shows that five samples were analyzed, but there are only experimental temperature values for the top three (since the pyrometer has a lower limit of 1400 °C). The values of the average particle size range from 2.66 to 5.54 μm for the 60 vol% TiNi composite, and from 1.92 to 2.58 μm for the 70 vol% TiNi composite. If we assume that we can extrapolate down to low temperatures for the latter composite, as was done in Fig. 5, then the particle size at a temperature of 1400 °C would be around 0.52 μm.

Fig. 6 shows a plot of the average particle size of TiC as a function of location along the length of several 60 vol% TiNi samples. Three of the samples, marked with maximum combustion temperatures of 1604, 1714 and 1861 °C, are standard samples reacted with applied fields of 0, 1.54 and 3.91 V cm^{-1}, respectively. The other two samples, marked with maximum combustion temperatures of 1787 and 1836 °C, were samples that had the electric field (5.58 and 7.74 V cm^{-1}) only at the beginning of the reaction; the field was turned off about 2 s into the reaction. The maximum combustion temperatures shown in Fig. 6 are the temperatures measured by the pyrometer, which is focused on the center of the sample.

4. Discussion

The rate of propagation of a combustion wave through the reactant mixture is dictated by thermophysical and heat transfer criteria. On the assumption that convective and radiative heat losses are negligible and that the field contribution is primarily thermal, the following expression describes the energy balance for this case [5]:

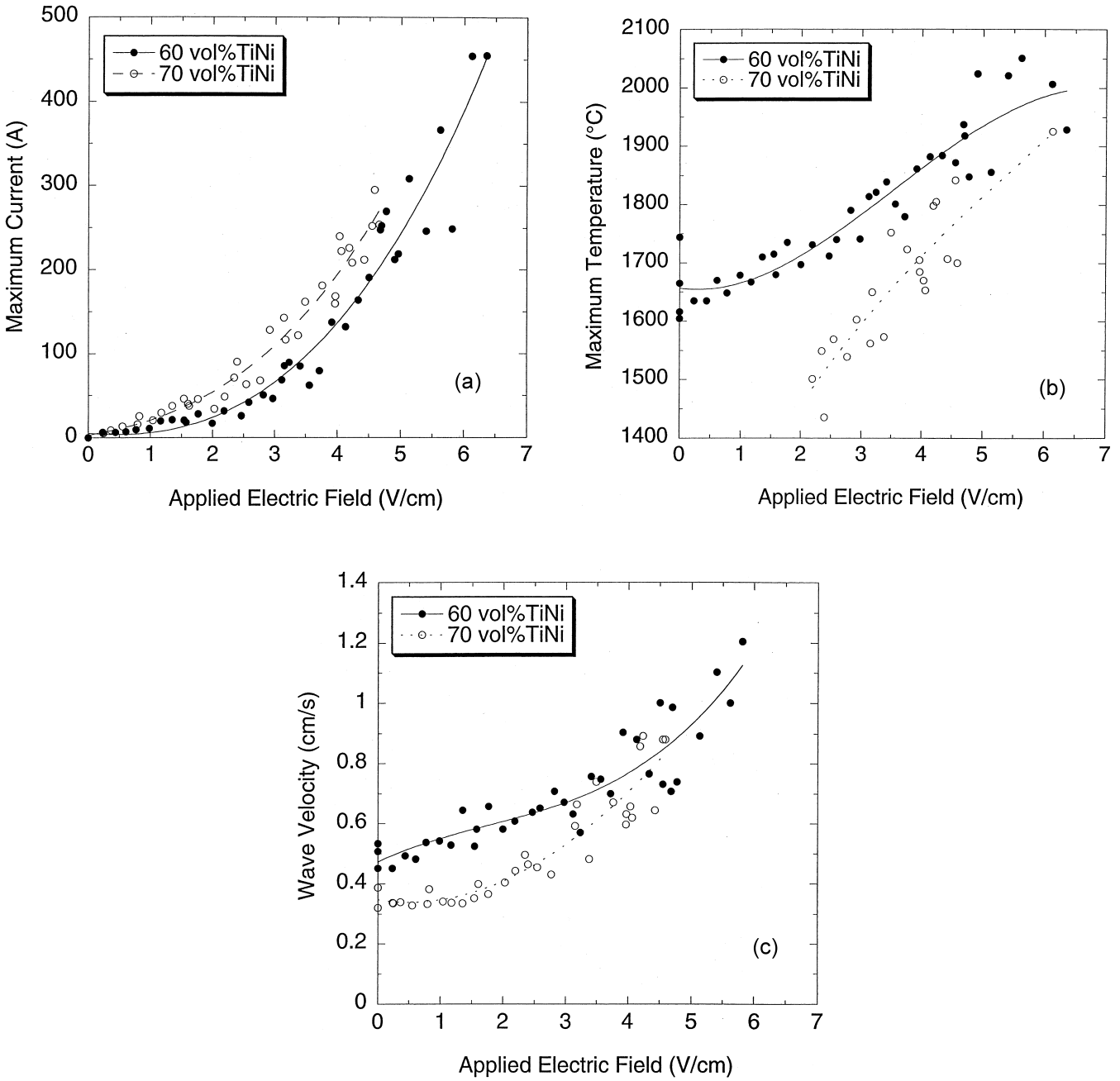

Fig. 1. Dependence of (a) the maximum current, (b) the maximum combustion temperature and (c) the wave velocity on the applied electric field.

$$\rho C_{\mathrm{p}} \frac{\partial T}{\partial t} = \nabla \cdot (\kappa \nabla T) + H \frac{1}{z} \frac{\partial \gamma_z}{\partial t} + \sigma |\nabla \upsilon|^2 - 2 \frac{\sigma_{\mathrm{B}} (T^4 - T_{\mathrm{o}}^4)}{w} \tag{3}$$

where ρ is the density of the sample; C_{p} is the heat capacity of the mixture (which can be calculated as the average of the heat capacities of the components, weighted by the mole fraction of each component); T is temperature; t is time, κ and σ are, respectively, the thermal and electrical conductivities of the mixture, υ is the electrostatic potential, σ_{B} is the Stefan-Boltzmann constant, T_{o} is the ambient temperature around the sample, and w is the width of the sample in the third dimension. The rate of heat accumulation in the reaction front (the left-hand side in Eq. (3)) is the sum of the rates of net heat conduction, heat of reaction, and Joule heat.

The chemical heat generation term in Eq. (3) is based on a stoichiometric equation of the form $xX + yY \rightarrow zZ + H$, with H being the enthalpy of the reaction, z is the stoichiometric coefficient of the product, and γ_z is the molar fraction per cubic centimeter of the product. The term $\partial \gamma_Z / \partial t$ is described by,

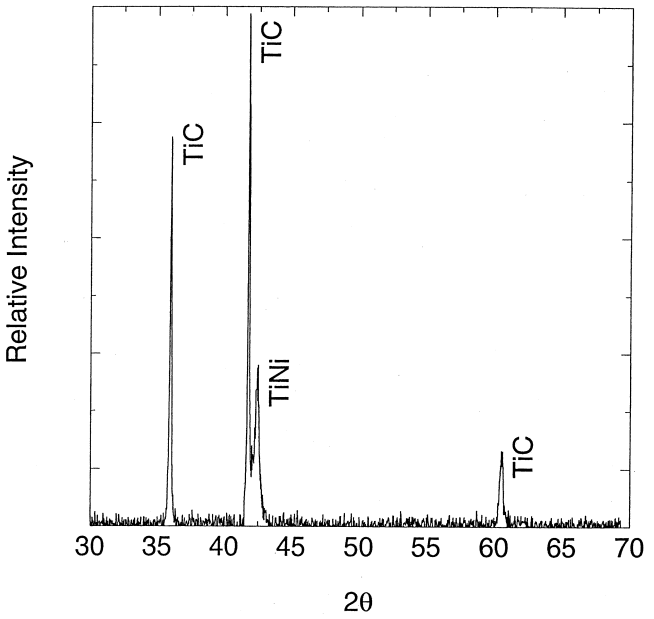

Fig. 2. A typical XRD pattern for a TiNi–TiC composite obtained by combustion synthesis.

$$\frac{\partial \gamma_Z}{\partial t} = \mathrm{d}\gamma_X \gamma_Y K \exp\left(-\frac{E_a}{RT}\right) \quad (4)$$

here, K is the pre-exponential constant, E_a is the activation energy of the reaction, R is the universal gas constant, and γ_X and γ_Y, are the mole fractions of the reactants per unit volume. From Eqs. (3) and (4), and assuming Arrhenius (chemical) kinetics, an expression for the rate of propagation is reported in the following form [22]:

$$\ln\left(\frac{u}{T_c}\right) = -\frac{E_a}{2RT_c} + \frac{\ln\left[b\left(\frac{R}{E_a}\right)\right]}{2} \quad (5)$$

where u is the wave velocity, T_c is the combustion temperature, and b is a constant. By obtaining a plot of $\ln(u/T_c)$ versus $1/T_c$, the activation energy for the reaction can be obtained. Such plots for the TiNi–TiC (60 and 70 vol% TiNi) composites are shown in Fig. 7. The calculated apparent activation energies for the two cases are 107 and 100 kJ mol^{-1}, respectively.

As indicated in Section 1, aside from other, less investigated effects such as electromigration, the imposition of a field has a thermal influence through Joule heating. The degree of activation by Joule heating depends on the spatial distribution of the current, which in turn depends on the temperature dependence of the electrical conductivities of reactants and product phases [23]. The observed increase in both temperature and wave velocity is expected to provide steeper temperature gradients, as seen in Fig. 8 for values obtained from the advancing front of the wave. The higher gradients are expected to lead to a decrease in the total reaction time. This can be seen in Fig. 9a,b. This leads to expectations of a lesser tendency for grain growth in the product. However, the results obtained in this study for the two compositions investigated, show that particles increased in size significantly with an increase in field strength (Fig. 5). In both TiNi–TiC composites we can see that particle coarsening is not negligible. The average particle size of TiC with no applied field is around 2 μm. With a high field, the average particle size is a factor of three higher, about 6 μm.

This increase is viewed in terms of the presence of a molten phase, in which higher values of mass transport parameters are realized. The amount of molten phases should also have an effect on the particle size. In a study on WC–Co cermets, it was shown that the coarsening of WC grains is enhanced with an increase in the liquid content in the compacts [24]. The maximum amount of molten phase that can be obtained for the 60 and 70 vol% TiNi composites is 84.8 and 88.3 vol%, respectively. These amounts are calculated on the basis that the combustion temperature is higher than the melting temperatures of both Ni and Ti. Fig. 1b shows that these temperatures are exceeded for many of the samples reacted. During the reaction, the availability of greater amounts of molten phases should promote particle coarsening, as diffusion of matter from the small particles to the large particles is facilitated. Fig. 10 shows a plot of the time during which the reactions were at temperatures above 1455 °C (the melting temperature of Ni, the higher of the two metals). The figure shows that the 60 vol% TiNi composite stayed above 1455 °C for 2.5–3.0 s while the corresponding time for the 70 vol% TiNi was 1–2 s. The plot also shows that the coarsening time increases with an increase in the applied field, although the increase is not very pronounced.

From these results, one expects that the grain size of the 60 vol% TiNi composites to be larger than that of the 70 vol% composites since the former has higher temperatures and the time at which the temperatures are higher than the melting point of Ni is longer. These expectations are supported by the results presented in Fig. 5. In the presence of a liquid phase, higher temperatures gradients at the wave front do play an important role, as they were reported to do in other situations [11]. In another study, in a system where no molten phase is present during synthesis (the formation of TaC), the increase in the field strength, with its concomitant increase in the temperature gradient, has a relatively small influence on grain size until the temperature reaches the melting point of Ta. These results will be reported in a subsequent paper [25].

As mentioned in Section 3, Fig. 6 shows a plot of the average particle size at locations across the length of several 60 vol% TiNi samples. Although the initial fields are relatively high for the samples which experienced a removal of the field, the measured temperatures are lower since these values were obtained in the middle of the sample. The average particle size is higher at the beginning of the sample because of the combined effect of the field

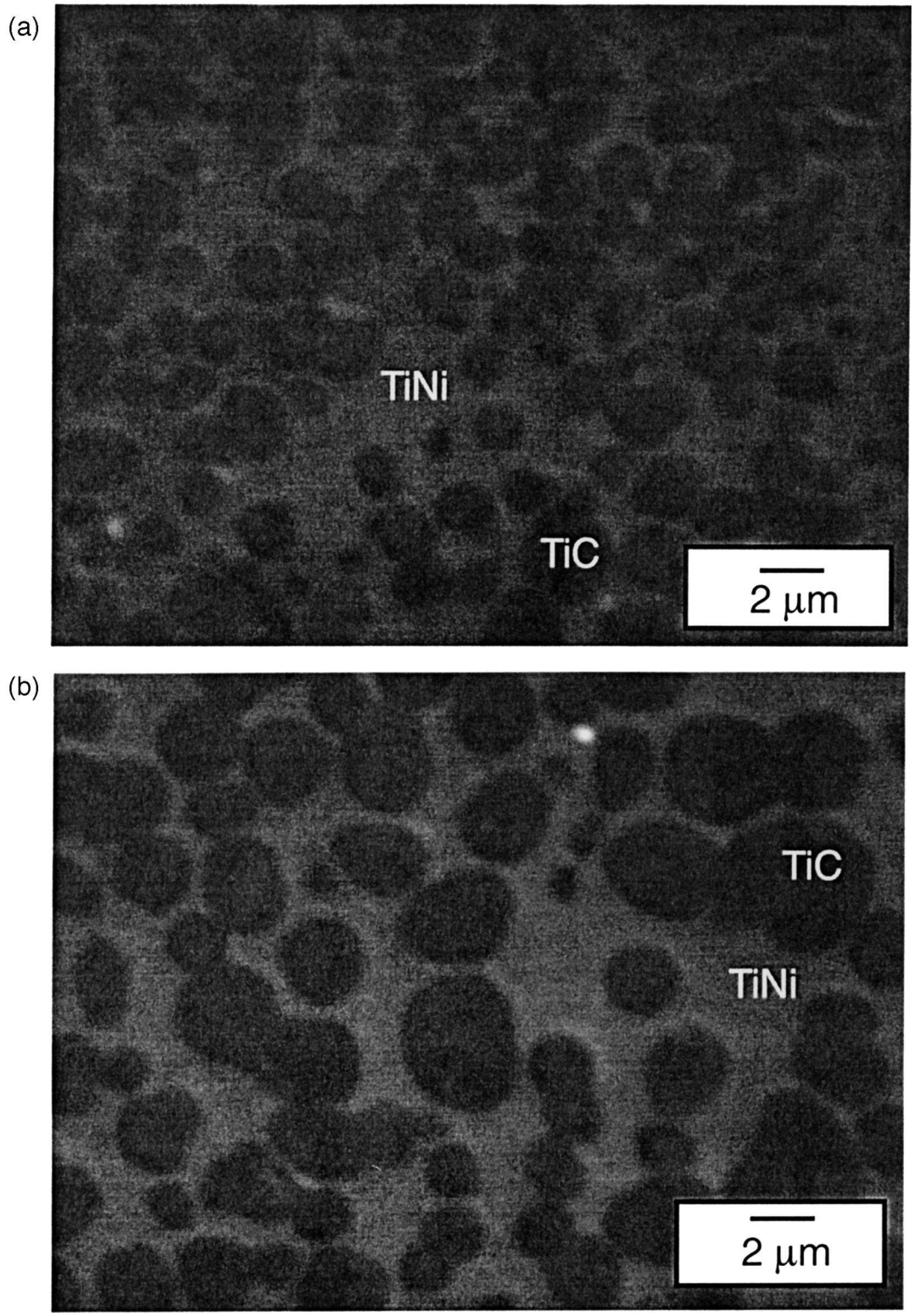

Fig. 3. Micrograph of a TiNi–TiC composite reacted (a) without an electric field and (b) reacted with an applied electric field of 5.82 V cm^{-1}.

and the ignition source energies. Away from the edge of the sample, the particle size correlates generally well with the measured temperature, as can be seen from Fig. 6. Larger particle size gradients were seen in the samples in which the field was turned off, consistent with anticipated temperature gradients in these samples. If the electric field had not been turned off, the maximum combustion temperature and the particle size would have been higher.

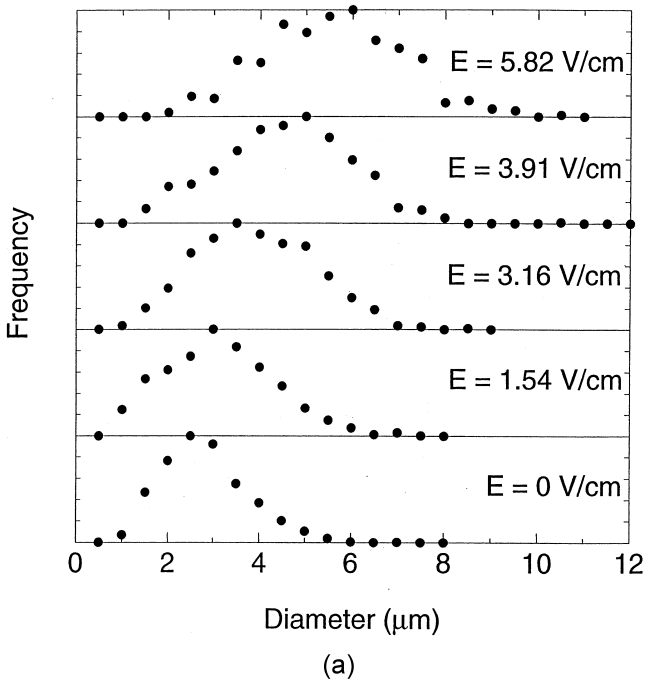

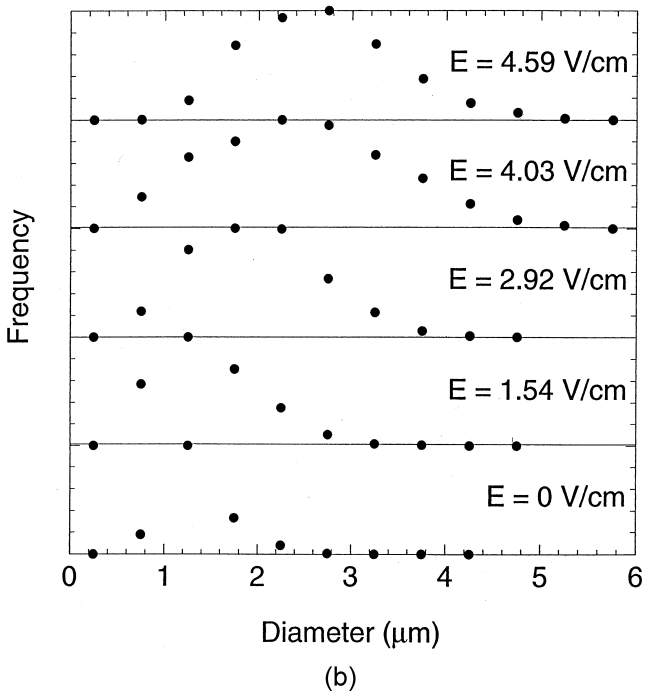

Fig. 4. TiC particle size distribution for (a) the 60 vol% TiNi composite and (b) for the 70 vol% TiNi composite.

Furthermore, the particle size would have been relatively more uniform, as in the case of the first three samples.

5. Summary

The effect of an electric field on the microstructural development during the combustion synthesis of TiC–TiNi composites was investigated. Using elemental reactants, composites containing 60 and 70 vol% TiNi were synthesized under different field conditions. The imposition of a field increased the maximum reaction temperature and the combustion wave velocity. An increase in field is consistent with an increase in the relative amount of a molten phase. The length of time at which the temperature is higher than the melting point of nickel increased with increasing field. The result of this is an increase in the

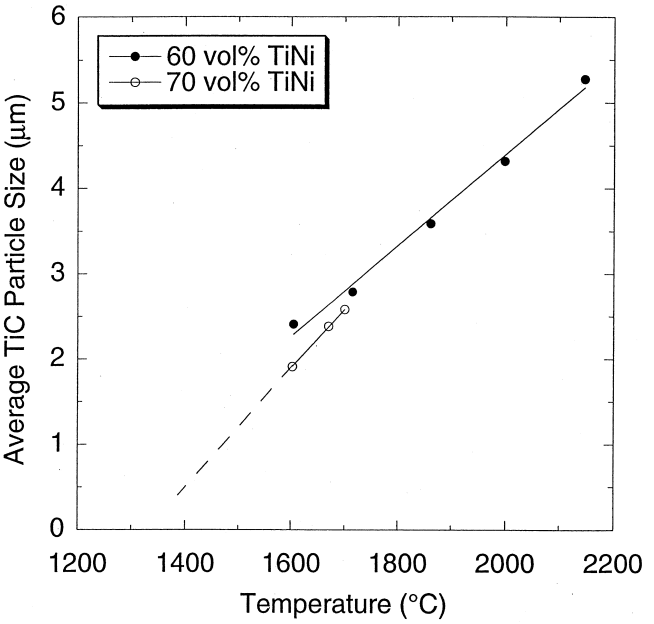

Fig. 5. Effect of temperature on average particle size of TiC for the TiNi–TiC composites.

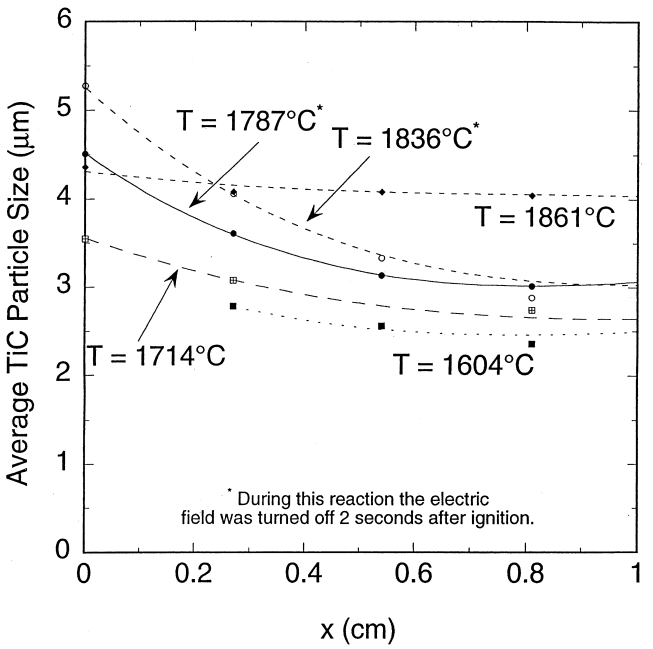

Fig. 6. Dependence of the average particle size of TiC on location along sample of several 60 vol% TiNi composites.

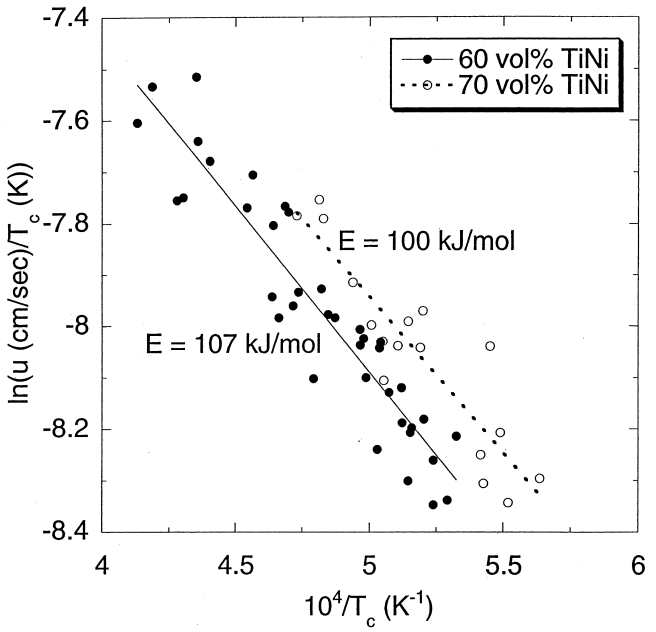

Fig. 7. Arrhenius plot of $\ln(u/T_c)$ versus $1/T_c$ for the TiNi–TiC composites.

particle size of the TiC component with an increase in the strength of the field. For both the 60 and 70 vol% TiNi samples, the particle size of TiC increased by at least a factor of two as the field increased from zero to about 5 V cm^{-1}. Although higher temperatures and wave velocities result in higher temperature gradients and thus an anticipation of shorter residence time at the highest temperatures, the presence of a liquid phase has apparently a more direct

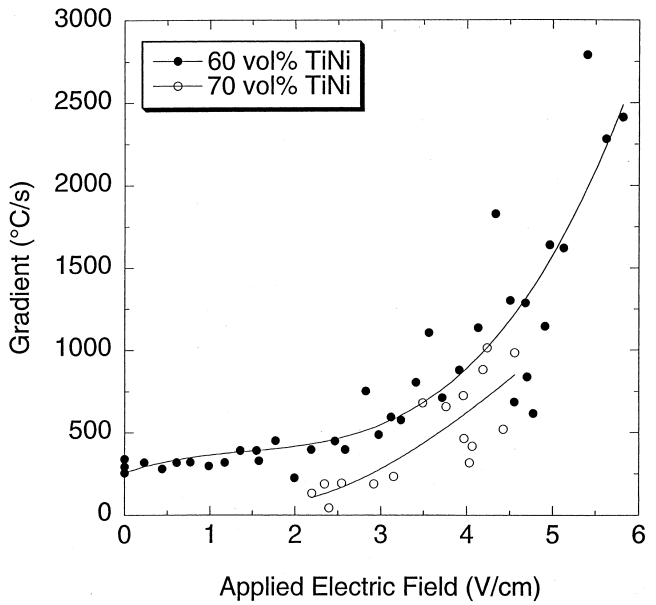

Fig. 8. Temperature gradients for the TiNi–TiC composites.

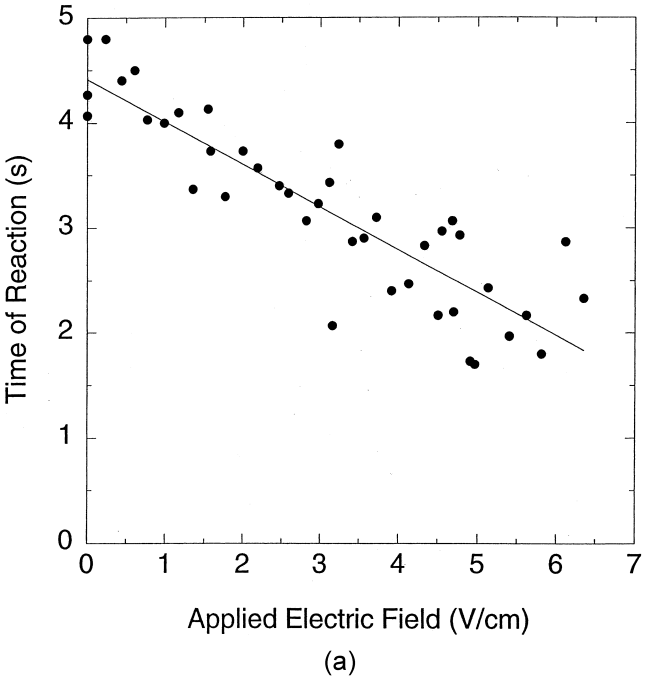

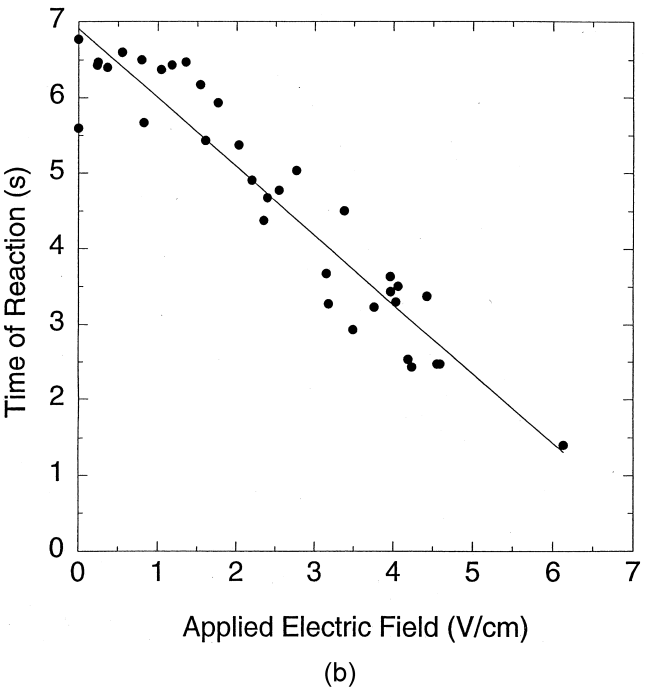

Fig. 9. Combustion times for (a) the 60 vol% composite and (b) for the 70 vol% TiNi composite as functions of applied field.

effect on TiC particle growth. In cases where no liquid is present the results are different, as will be reported in a subsequent paper [25].

From wave propagation dynamics, the activation energies for the formation of the 60 and 70 vol% TiNi composites were determined as 107 and 100 kJ mol^{-1}, values which are in reasonable agreement with the previ-

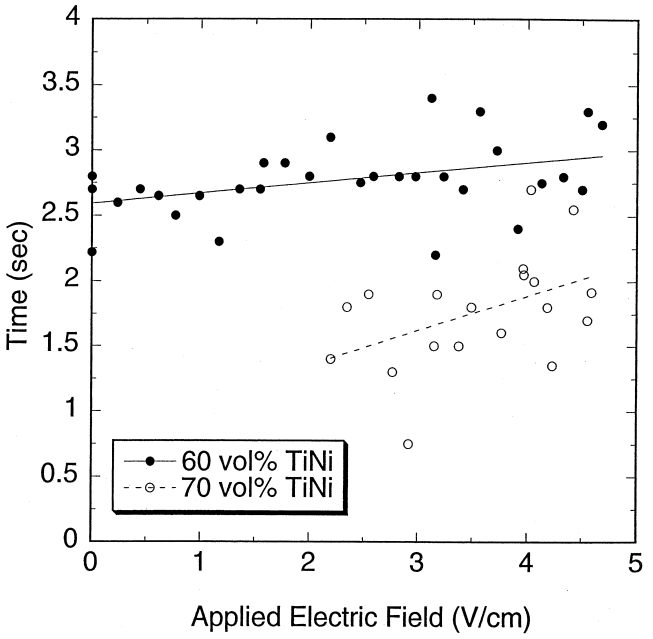

Fig. 10. Time during which the TiNi–TiC reaction was above 1455 °C versus applied electric field.

ously reported value by Dumnead et al. [15] of 133±50 kJ mol^{-1} for the formation of TiC–Ni composites.

Acknowledgements

This work was supported by a grant from the National Science Foundation.

References

[1] Z.A. Munir, Z. Phys. Chem. 207 (1998) 39–57.
[2] Z.A. Munir, W. Lai, K. H. Ewald, US Patent No. 5,380,409, 10 January 1995.
[3] Z.A. Munir, Int. J. SHS 6 (1997) 165–185.
[4] Z.A. Munir, Mater. Sci. Eng. A287 (2000) 125–137.
[5] A. Feng, Z.A. Munir, Metall. Trans. 26B (1995) 581–586.
[6] N. Bertolino, J. Garay, U. Anselmi-Tamburini, Z.A. Munir, Scripta Mater. 44 (2001) 737–742.
[7] A. Feng, Z.A. Munir, Metall. Trans. 26B (1995) 587–593.
[8] K. Kawase, Z.A. Munir, Int. J. SHS 7 (1998) 95–102.
[9] R. Orru, G. Cao, Z.A. Munir, Metal. Mater. Trans. 30A (1999) 1101–1108.
[10] H. Xue, Z.A. Munir, J. Eur. Ceram. Soc. 17 (1997) 1787–1792.
[11] Z.A. Munir, in: Molybdenum and Molybdenum Alloys, A. Crowson, E.S. Chen, J.A. Shields, P.R. Subramanian (Eds.), Proceedings of TMS Symposium, Warrendale, PA, 1998, pp. 49–60.
[12] J.Y. Huang, L.L. Ye, Y.K. Wu, H.Q. Ye, Metall. Mater. Trans. A 26 (1995) 2755–2759.
[13] J.Y. Huang, L.L. Ye, Y.K. Wu, H.Q. Ye, Acta Mater. 44 (1996) 1781–1792.
[14] H.Z. Ye, R. Liu, D.Y. Li, R. Eadie, Scripta Mater. 41 (1999) 1039–1045.
[15] S.D. Dunmead, D.W. Readey, C.E. Semler, J.B. Holt, J. Am. Ceram. Soc. 72 (1989) 2318–2324.
[16] M.J. Capaldi, J.V. Wood, J. Mater. Synth. Process. 4 (1996) 245–253.
[17] J. Wong, E.M. Larson, J.B. Holt, P.A. Waide, B. Rupp, R. Frahm, Science 249 (1990) 1406–1409.
[18] A.S. Rogachev, V.M. Shkiro, I.D. Chausskaya, M.V. Shvetsov, Combust. Explos. Shock Waves 24 (1988) 720–726.
[19] J.C. LaSalvia, M.A. Meyers, D.K. Kim, J. Mater. Synth. Process. 2 (1994) 255–274.
[20] J.C. LaSalvia, D.K. Kim, M.A. Meyers, Mater. Sci. Eng. A206 (1996) 71–80.
[21] J.C. LaSalvia, M.A. Meyers, Int. J. SHS 4 (1995) 43–57.
[22] Z.A. Munir, U. Anselmi-Tamburini, Mater. Sci. Rep. 3 (1989) 277–365.
[23] E.M. Carrillo-Heian, O.A. Graeve, A. Feng, J.A. Faghih, Z.A. Munir, J. Mater. Res. 14 (1999) 1949–1958.
[24] S. Kim, J.K. Park, D. Lee, Scripta Mater. 38 (1998) 1563–1569.
[25] O.A. Graeve, Z.A. Munir, J. Mater. Res. (2002) in press.